The phase diagram of the Lennard-Jones fluid using temperature dependent interaction parameters

Ali Kh. Al-Matar[a]; Ahmed H. Tobgy[a]; Ibrahim A. Suleiman[a]

[a] Chemical Engineering Department, Faculty of Engineering and Technology, University of Jordan, Amman, Jordan

PLEASE SCROLL DOWN FOR ARTICLE

Taylor & Francis
Taylor & Francis Group

The phase diagram of the Lennard-Jones fluid using temperature dependent interaction parameters

Ali Kh. Al-Matar*, Ahmed H. Tobgy and Ibrahim A. Suleiman

Chemical Engineering Department, Faculty of Engineering and Technology, University of Jordan, Amman, Jordan

The forces of interaction between argon atoms can be described by the Lennard-Jones potential model. It is hypothesised that the use of temperature dependent interaction parameters, instead of using temperature independent interaction parameters, may lead to improvement in the prediction of the vapour–liquid coexistence curve. Published second virial coefficient data were used to fit a simple two-parameter temperature dependent model for the collision diameter and well depth. Vapour–liquid coexistence curve for argon was simulated in the NVT Gibbs ensemble Monte Carlo technique. The simulations were carried out using each of the temperature independent and temperature dependent parameters in the temperature range: 110–148 K. The critical temperature and density were determined using the Ising-scaling model. The results using temperature dependent parameters produce, overall, a more accurate phase diagram compared to the diagram generated using temperature independent interaction parameters. The root mean square deviation is reduced by 42.1% using temperature dependent interaction parameters. Also, there was no significant difference between the results obtained using temperature dependent interaction parameters and the highly accurate and computationally demanding phase diagrams based on three body contributions.

Keywords: Gibbs ensemble; Lennard-Jones; phase diagram; critical constants; temperature-dependent

1. Introduction

Prediction and estimation of fluid phase equilibria are of crucial importance in the process industries. They find many applications in the design of chemical plants, rating of existing units as well as process and product R&D. Therefore, it is important to be able to understand the phase behaviour of pure liquids as a prerequisite to understanding mixtures phase behaviour.

Several models are available for modelling the intermolecular forces [1–5]. The Lennard-Jones model is the *de facto* standard in molecular simulations. Therefore, it is used in this work. The main proposition in this research is that introducing temperature dependent interaction parameters for the Lennard-Jones potential (collision diameter σ and well depth ε) instead of the current practice of using temperature independent interaction parameters, may lead to improvement in the prediction of phase equilibria. It should be emphasised that this approach is empirical in nature and does not entail any first principles justification. This study, aims at generating the phase diagram of argon, represented by the Lennard-Jones fluid, using temperature dependent interaction parameters. These parameters can be estimated using available compilation of the second virial coefficient [6,7]. Subsequently, a comparison of the

critical points based on the two types of generated phase diagram and available literature data and diagrams [8–13] will be carried out.

There are few recent studies on fitting temperature dependent parameters to certain compounds pertinent to heavy gases such as WF_6 and MoF_6 besides globule gases [14–19]. Nevertheless, these studies were limited to fitting of second virial coefficients and none of these studies dealt with generating the vapour–liquid coexistence curve. However, there was an attempt by Smit *et al.* [20] to model the phase behaviour using density dependent interaction parameters for the Lennard-Jones potential.

2. Intermolecular potential and simulation details

2.1 Intermolecular potential

The Lennard-Jones intermolecular potential model is used to represent the pair interaction between Argon atoms i and j separated by a distance r_{ij}:

$$u(r_{ij}) = 4\varepsilon_{ij} \left[\left(\frac{\sigma_{ij}}{r_{ij}} \right)^{12} - \left(\frac{\sigma_{ij}}{r_{ij}} \right)^{6} \right]. \quad (1)$$

The values of the collision diameter σ_{ij} (Å) = 3.405 and well depth ε_{ij}/k (K) = 125.2 [1] are used to represent temperature independent interaction parameters.

*Corresponding author. Email: aalmatar@ju.edu.jo

Interaction parameters as a function of temperature were determined from an optimisation process based on minimising the least squares of the error, calculated by comparing the experimental values for the second virial coefficient [7] and those determined using the following equation for the classical second virial coefficient:

$$B_{\text{classical}} = -2\pi N_A \int_0^\infty \left[e^{-u(r)/kT} - 1 \right] r^2 \, dr. \quad (2)$$

This is a nonlinear optimisation problem. Modified Marquardt–Levenberg method [21,22] was used to solve this problem. The objective function is to minimise the root mean square deviation (RMSD) value, where the RMSD is defined as:

$$\text{RMSD} = \sqrt{\frac{1}{N} \sum_{i=1}^{N} (B_{i,\text{exp}} - B_{i,\text{cal}})^2} \quad (3)$$

and, N is the number of observations, $B_{i,\text{exp}}$ is the experimental second virial coefficient for the ith observation and $B_{i,\text{cal}}$ is the calculated second virial coefficient for the ith observation. The integral was evaluated using a 21-point Gauss–Kronrod quadrature [22] to estimate the integral and the associated errors.

Only two-parameter relationships between the independent variable (temperature) and the dependent variables (σ and ε/k) were attempted. The relationships involved combination of linear, reciprocal, exponential and reciprocal–exponential terms [23]. Many of the attempted forms are found in the thermodynamic literature, such as exponential forms. Some optimised parameters were rejected based on physical reasoning. Only models with parameters that cause σ to increase with temperature and, ε/k to decrease with temperature were considered feasible [19]. The feasible models were subjected to a model discrimination process based on calculating posterior probability [24]. The selected model for the collision diameter and well depth as a function of temperature for argon are given by the following two equations [23]:

$$\sigma_{ij} = 3.672 - 22.30/T \quad (4)$$

$$\frac{\varepsilon_{ij}}{k} = 117.655 + 778.012/T. \quad (5)$$

Within the temperature range of interest for argon [110–148 K], used in the simulations which were carried out, the value of σ changes between 3.47 and 3.52 Å, while the value of ε_{ij}/k (K) changes in the range 124.7–122.9 K. These values are in general agreement with available temperature independent values [1,3].

3. Simulation details

Gibbs ensemble is used to simulate the coexistence of vapour and liquid phases. Systems of size 500 atoms were studied to simulate the vapour and liquid phases. All simulations were carried out with a spherical potential truncation for separations greater than 2.5σ and tail corrections included. The vapour–liquid simulations were started using two boxes with simple cubic lattice and the number of atoms was equally partitioned between the two boxes. The temperature of the entire system is held constant and surface effects are avoided by placing each box at the centre of a periodic array of identical boxes. The equilibration and production periods consisted of at least 200 and 2000 cycles, respectively. The type of Monte Carlo move was selected at random according to the following probabilities: 0.9089 translation, 0.0909 particle swap and 0.0002 volume exchange with one volume exchange per cycle.

The results generated for both phases, vapour and liquid, from the simulations are: energy, pressure, density, chemical potential and number of atoms in both boxes. The uncertainties in the ensemble averages were calculated by dividing the post-equilibrium results into ten blocks then taking the grand average [4]. The code employed in this work is developed in-house using object oriented programming in FORTRAN-90 and is available upon request.

4. Critical constants

Near the critical region, the free energy differences between two phases are small and as a result, Gibbs ensemble simulation becomes unstable. According to the scaling law, in the case of Gibbs ensemble simulation, the critical temperature is evaluated by the calculated $\rho - T$ coexistence data [25]:

$$\rho_L - \rho_v = b(T_c - T)^\gamma \quad (6)$$

where, γ is the non-classical 3D Ising critical exponent, $\gamma \approx 0.325$ and b and the critical temperature T_c are calculated from the fit. Subsequently, the critical density ρ_c can be determined using a fit based on the law of rectilinear diameters [25]:

$$\frac{\rho_L + \rho_v}{2} = \rho_c + A(T_c - T) \quad (7)$$

where, A and the critical density ρ_c are calculated from the fit.

5. Results and discussion

The second virial coefficient data was fitted using temperature independent interaction parameters as well as temperature dependent forms [23]. Figure 1 gives the residuals for the second virial coefficient data of argon using the values available in the literature [1], the optimised constants in this work (σ_{ij} (Å) = 3.507 and well depth ε_{ij}/k (K) = 117.26) and the fitted temperature dependent values: $\sigma_{ij} = 3.672 - 22.30/T$ and $\varepsilon_{ij}/k = 117.655 + 778.012/T$.

The calculated values of second virial coefficient using the new optimised constants are closer to experimental values. The parameters reported in Hirschfelder *et al.* [1], and which are widely used in the literature, yield a RMSD of 0.509 while the new optimised constants have a RMSD of 0.331. It should be noted, however, that although the RMSD has been reduced significantly, the residuals still show systematic trends suggesting that the temperature independent parameters are inadequate to describe the behaviour of the second virial coefficient over a wide temperature range.

It is clear that temperature dependent parameters produce more accurate results compared to temperature independent interaction parameters. The improvement is clear as the difference between experimental and calculated values decreases in temperature dependent cases and gets closer to the zero line than temperature independent case or even the optimised constant case. The gain in accuracy as measured by the RMSD is about 15 folds compared to the literature values and about 10 folds compared to the new optimised values. Moreover, the RMSD for the temperature dependent interaction

models are in a narrow band of width ± 1 cm³/mol which are within the Class I classification of Dymond and Smith [6]. The temperature independent models do not reduce the RMSD to this band implying their inadequacy.

Figure 2 compares the vapour–liquid coexistence curve for simulation using temperature independent interaction parameters from Panagiotopoulos et al. [9], this work at the same conditions using temperature independent interaction parameters taken from the literature [1] and temperature dependent interaction parameters in this work. Also, the same figure shows the three body simulation results of Sadus and Prausnitz [10] and experimental data for argon from Gilgen et al. [26]. The calculated results are shown in lines, while experimental data are given as symbols. A summary of the results using temperature dependent interaction parameters is given in Table 1.

The results of Panagiotopoulos *et al.* [9] and those using temperature independent parameters are close to each other, which is reasonable as both are using the same methodology and temperature independent interaction parameters. Simulations using temperature independent interaction parameters in this work are slightly closer to the experimental data compared to previous work which may be attributed to longer runs and the number of configurations generated.

It is clear from Figure 2 that the vapour–liquid coexistence curve generated using temperature dependent interaction parameters is much closer to the experimental values compared to the temperature independent interaction parameters' curve and the curve of Panagiotopoulos *et al.* [9]. This improvement
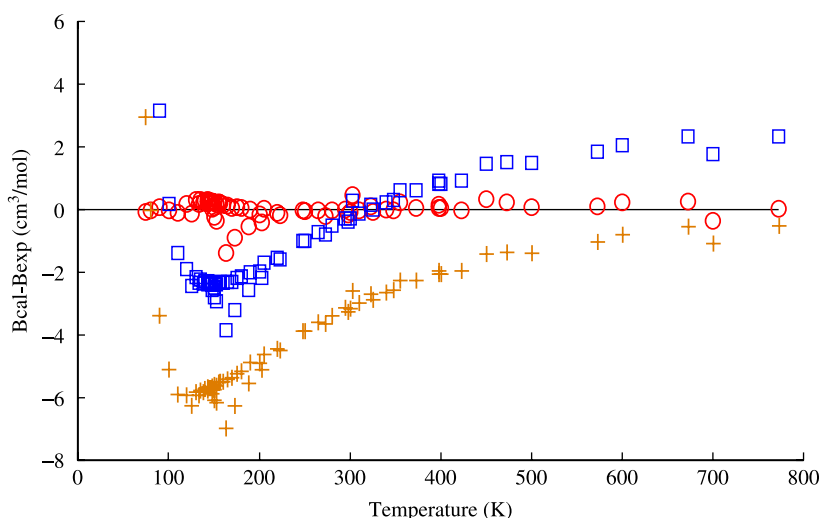

Figure 1.   Residuals between experimental second virial coefficient and calculated second virial coefficient for argon: + temperature independent (literature values taken from Hirschfeleder *et al.* [1]), □ temperature independent (this work), ○ temperature dependent (this work).
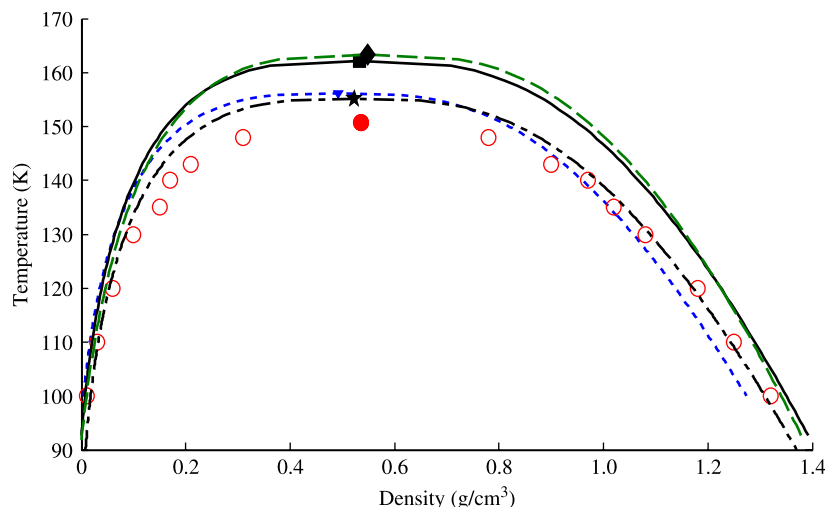
Figure 2.   Vapour–liquid coexistence curve for argon: ○ experimental data (Gilgen *et al.* [26]), – – – (Panagiotopoulos *et al.* [9]), —— temperature independent (this work), –.–.– three body Axilrod–Teller (Sadus and Prausnitz [10]) and … … temperature dependent (this work). ● Experimental critical point, ◆ Panagiotopoulos *et al.* [9]) critical point, ■ temperature independent (this work) critical point, ∗ (Sadus and Prausnitz [10]) critical point, ▼ temperature dependent critical point (this work).

is particularly evident for the density of the liquid phase with marginal improvement for the vapour phase away from the critical region. However, there is significant improvement for the shape of the curve near the critical region. The RMSD values were calculated from the experimental density data in the temperature range [100–150] K. Simulation using temperature dependent interaction parameters improved the value of critical temperature. It is closer to the experimental value by 3.3%. However, simulation using temperature dependent interaction parameters worsen the value of critical density placing it farther from experimental value by 7.6%. This may be attributed to the fact that the Lennard-Jones potential with temperature independent interaction parameters overestimates the attractive forces. While the use of temperature dependent interaction parameters reduce the well depth and widen the region around it resulting in a reduction in the magnitude of attractive forces. The reduction in the magnitude of the attractive forces is more pronounced for the liquid phase. It should be noted that there is significant improvement for the shape of the curve near the critical region. This

improvement is evident by comparing the RMSD of the temperature dependent interaction parameters ($77 \, \text{kg/m}^3$) compared to that of the temperature independent interaction parameters ($133 \, \text{kg/m}^3$), which is equivalent to a reduction of RMSD by 42.1%. This reduction in the RMSD provides a further evidence of the success of using temperature dependent interaction parameters.

The coexistence curves using temperature dependent interaction parameters and three body effects are close to each other; with the results of Sadus and Prausnitz [10] being slightly better overall. This is not surprising since Sadus and Prausnitz used the Axilrod–Teller approximation to account for three body interactions which is more physically accurate representation of the actual molecular interaction among the molecules, compared to pairwise interactions. However, the inclusion of this more realistic model is expensive in terms of computational time required. It is worth mentioning that they used a CRAY C90 processor and the run took 2 h of CPU time [10] for a system of 300 molecules, while a typical run of a system consisting of 500 atoms required 3.5 h of CPU time on a PC with 3 GHz processor

Table 1.   Coexistence energies, pressures and densities, and their associated standard deviations, of pure LJ fluid as represented by argon for different temperatures at a total number of atoms $N = 500$.

Temperature	Energy (J/mol)		Pressure (bar)		Density (g/cm^3)	
	Liquid	Vapour	Liquid	Vapour	Liquid	Vapour
110	−5656.4 ± 24.3	−145.7 ± 95.3	4.246 ± 18.21	4.155 ± 0.74	1.220 ± 0.004	0.020 ± 0.002
120	−5226.9 ± 28.0	−231.6 ± 69.0	7.854 ± 17.84	7.376 ± 0.89	1.128 ± 0.005	0.034 ± 0.002
135	−4610.6 ± 34.3	−502.3 ± 48.9	16.790 ± 15.27	17.593 ± 1.37	1.002 ± 0.005	0.082 ± 0.003
143	−4282.5 ± 42.3	−729.0 ± 54.3	30.047 ± 14.43	26.102 ± 1.97	0.929 ± 0.006	0.127 ± 0.004
148	−4018.3 ± 58.1	−944.2 ± 74.5	35.386 ± 13.85	32.083 ± 2.53	0.869 ± 0.008	0.168 ± 0.006

Table 2. Critical constants for argon using various approaches.

	ρ_c (kg/m^3)	T_c (K)	RMSD[†] (kg/m^3)
Experimental [26]	535.6	150.687	–
Temperature independent interaction parameters [9]	548.6	163.392	133
Temperature independent interaction parameters (this work)	532.7	162.149	130
Temperature dependent interaction parameters (this work)	491.8	156.087	77
Three body effects using Axilrod–Teller [10]	522.6	155.088	69

[†] RMSDs are calculated all over temperature range with number of data points = 26.

using temperature dependent interaction parameters. Therefore, using temperature dependent interaction parameters provides a saving in the computational resources in terms of hardware and time while not sacrificing accuracy. The reduction of RMSD values for the simulation using three body interactions is about 48.1%, while using temperature dependent interaction parameters reduces the RMSD by 42.1%. The gain in accuracy may not justify the computational cost. Table 2 summarises the critical constants and the RMSD for the various approaches discussed in this paper. The RMSD values were calculated from the experimental density data in the temperature range [100–150] K.

Figure 3 gives the vapour pressure versus temperature curves obtained from vapour phase results using temperature dependent interaction parameters. This figure compares temperature dependent interaction parameters results, the results of Nasrabad [12] and the experimental vapour pressure data, as fitted by Antoine equation, for argon. The results are close to each other while the results of Nasrabad [12,13] requires more efforts and computational cost as he used Aziz and Salman and his *ab initio* models (av5z and av45z) plus three body interactions using the Axilrod–Teller

approximation. Table 3 also shows the RMSD in vapour pressure values of argon using temperature independent interaction parameters. This table shows that a reduction in the RMSD value of 5.7% is achieved using temperature dependent interaction parameters compared to the RMSD values using temperature independent interaction parameters. This reduction is marginal compared to the reduction achieved using three body interactions [12,13], amounting to 75.5%.

6. Conclusions

The concept of temperature dependent interaction parameters for argon modelled as a Lennard-Jones fluid is introduced. This concept was used to fit the collision diameter and well depth as a function of temperature for argon. The concept was applied to second virial coefficient data and it was shown to be successful in reducing the RMSD by 15 folds compared to conventional temperature independent interaction parameters. Also, evidence is produced in this research that using temperature dependent interaction parameters indeed improves the simulated vapour–liquid coexistence curve of argon modelled as a Lennard-Jones fluid, and
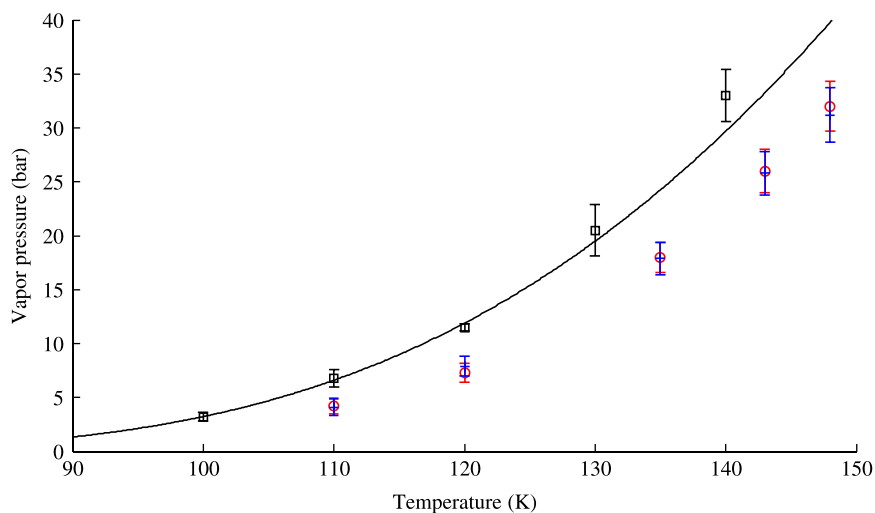

Figure 3. Vapour pressure of argon versus temperature: + temperature independent (this work), □ three body with Aziz–Salman potential (Nasrabad [12,13]) and ○ temperature dependent (this work).

Table 3. RMSD in vapour pressure of argon for cases of temperature independent interaction parameters, temperature dependent interaction parameters and Nasrabad [12].

	RMSD (bar)
Temperature independent interaction parameters (this work)	6.21
Temperature dependent interaction parameters (this work)	5.85
Three body effects using Axilrod–Teller [12]	1.43

potentially any phase diagram. Simulations using temperature dependent interaction parameters can generate phase diagrams closer to experimental phase diagram. The results based on the simulated vapour–liquid coexistence curve for argon in the temperature range (100–150) K using temperature dependent interaction parameters indicated that a reduction of 42.1% in the RMSD of density is achieved relative to the values generated using temperature independent interaction parameters. However, the predicted critical values were somewhat mixed; the predicted critical temperature was improved, while the opposite was true for the predicted critical density. The simulation results were roughly equivalent with the three body effects being slightly better at the expense of significantly increased computational demand. To use the approach of the current research for generating the phase diagrams of the binary and multicomponent mixtures of Lennard-Jones fluids is avenue that may be considered for further research to validate such an approach.

References

[1] J.O. Hirschfelder, C.F. Curtiss, and R.B. Bird, *Molecular Theory of Gases and Liquids, Second Corrected Printing*, John Wiley and Sons, New York, 1964.

[2] T.M. Reed, and K.E. Gubbins, *Applied Statistical Mechanics*, McGraw-Hill, New York, 1973.

[3] J.M. Prausnitz, R.N. Lichtenthler, and E.G. de Azevedo, *Molecular Thermodynamics of Fluid-phase Equilibria*, 3rd ed., Prentice Hall PTR, New Jersey, 1999.

[4] D. Frenkel, and B. Smit, *Understanding Molecular Simulation: From Algorithms to Applications*, 2nd ed., Academic Press, San Diego, 2002.

[5] D.C. Rapaport, *The Art of Molecular Simulation*, Cambridge University Press, Cambridge, 1995.

[6] J.H. Dymond and E.B. Smith, *The Virial Coefficients of Pure Gases and Mixtures: A Critical Compilation*, Clarendon Press, Oxford, 1980.

[7] J.H. Dymond *et al.*, *Virial Coefficients of Pure Gases and Mixtures, Subvolume A: Virial Coefficients of Pure Gases*, Springer-Verlag, Berlin, 2002.

[8] A.Z. Panagiotopoulos, *Direct determination of phase coexistence properties of fluids by Monte Carlo simulation in a new ensemble*, Mol. Phys. 61(4) (1987), pp. 813–826.

[9] A.Z. Panagiotopoulos *et al.*, *Phase equilibria by the simulation in the Gibbs ensemble: Alternative derivation, generalization and application to mixtures and membrane equilibria*, Mol. Phys. 63(4) (1988), pp. 527–545.

[10] R.J. Sadus and J.M. Prausnitz, *Three-body interactions in fluids from molecular simulation: Vapor–liquid phase coexistence of argon*, J. Chem. Phys. 104(12) (1996), pp. 4784–4787.

[11] R.J. Sadus, *Molecular simulation of the thermophysical properties of fluids: Phase behaviour and transport properties*, Mol. Simul. 32(3–4) (2006), pp. 185–189.

[12] A.E. Nasrabad, *Global simulation of noble gases and their binary mixtures*, Ph.D. dissertation, University of Köln, Köln, Germany, 2003.

[13] A.E. Nasrabad, R. Laghaei, and U.K. Deiters, *Prediction of the thermophysical properties of pure neon, pure argon, and the binary mixtures neon–argon and argon–krypton by Monte Carlo simulation using* ab initio *potentials*, J. Chem. Phys. 121(13) (2004), pp. 6423–6434.

[14] L. Zarkova and P. Pirgov, *Transport and equilibrium properties of UF_6 gas simultaneously fitted by an effective isotropic potential with temperature-dependent parameters*, J. Phys. B: At. Mol. Opt. Phys. 28(19) (1995), pp. 4269–4281.

[15] ———, *The isotropic temperature-dependent potential describing the binary interactions in gaseous WF_6 and MoF_6*, J. Phys. B: At. Mol. Opt. Phys. 29(19) (1996), pp. 4411–4422.

[16] L. Zarkova, P. Pirgov, and G. Paeva, *Simultaneously predicted transport and equilibrium properties of boron trifluoride gas*, J. Phys. B: At. Mol. Opt. Phys. 32 (1999), pp. 1535–1545.

[17] L. Zarkova and U. Hohm, *pVT-second virial coefficients B(T), Viscosity η(T) and self diffusion ρD(T) of the gases: BF_3, CF_4, SiF_4, CCl_4, $SiCl_4$, SF_6, MoF_6, WF_6, UF_6, $Cl(CH_3)_4$ and $Si(CH_3)_4$ determined by means of an isotropic temperature- dependent potential*, J. Phys. Chem. Ref. Data 31(1) (2002), pp. 183–216.

[18] L. Zarkova, U. Hohm, and M. Damyanova, *Viscosity and pVT-second virial coefficient of binary noble–globular gas and globular–globular gas mixtures calculated by means of an isotropic temperature-dependent potential*, J. Phys. Chem. Ref. Data 32(4) (2003), pp. 1591–1705.

[19] G. Parsafar, F. Kermanpour, and B. Najafi, *Prediction of the temperature and density dependencies of the parameters of the average effective pair potential using only the LIR equation of state*, J. Phys. Chem. B 103(34) (1999), pp. 7287–7292.

[20] B. Smit, T. Hauschild, and J.M. Prausnitz, *Effect of density-dependent potential on the phase behaviour of fluids*, Mol. Phys. 77(6) (1992), pp. 1021–1031.

[21] D. Marquardt, *An algorithm for least-squares estimation of nonlinear parameters*, SIAM J. Appl. Math. 11(2) (1963), pp. 431–441.

[22] W.H. Press *et al.*, *Numerical Recipes in Fortran: The Art of Scientific Computing*, 2nd ed., Cambridge University Press, Cambridge, 1992.

[23] I.A. Suleiman, *Vapor–liquid diagram of Lennard-Jones fluid using temperature dependent interaction parameters*, M.Sc. thesis, University of Jordan, Amman, Jordan, 2007.

[24] P.M. Berthouex and L.C. Brown, *Statistics for Environmental Engineers*, 2nd ed., CRC Press, New York, 2002.

[25] A.Z. Panagiotopoulos, *Molecular simulation of phase coexistence: finite size effects and determination of critical parameters for two- and three-dimensional Lennard-Jones fluids*, Int. J. Thermophys. 15(6) (1994), pp. 1057–1072.

[26] R. Gilgen, R. Kleinrahm, and W. Wagner, *Measurement and correlation of the (pressure, density, temperature) relation of argon. I. The homogeneous gas and liquid regions in the temperature range from 90 K to 340 K at pressures up to 12 MPa*, J. Chem. Thermodyn. 26 (1994), pp. 383–398.